Laser and Particle Beams (2010), *28*, 387–392.

doi:10.1017/S0263034610000339

Influence of laser beam intensity profile on propagation dynamics of laser-blow-off plasma plume

AJAI KUMAR,[1] SONY GEORGE,[2] R.K. SINGH,[1] AND V.P.N. NAMPOORI[2]

[1]Institute for Plasma Research, Gandhinagar, India
[2]ISP, Cochin University of Science and Tech., Cochin, India

(RECEIVED 28 January 2010; ACCEPTED 1 May 2010)

Abstract

Effect of intensity profile of the ablating laser on the dynamics of laser-blow-off (LBO) plume has been studied by fast imaging technique. This work emphasizes the geometrical aspect of the LBO plume, which is an important parameter for various applications. Visualization of the expanding plume reveals that geometrical shape and directionality (divergence) of the plume are highly dependent on the laser intensity profile. Present results demonstrate that the Gaussian profile laser produces a well-collimated, low divergence plasma plume as compared to the plume formed by a top-hat profile laser. The sequence of film removal processes is invoked to explain the role of energy density profile of the ablating laser in LBO mechanism.

Keywords: Influence of laser beam intensity profile; Laser-blow-off

INTRODUCTION

Generation of collimated laser ablated plasma plume is of great interest because of its importance in several fundamental and applied research areas. It can play a crucial role in the development of extreme ultraviolet lithography source, thin film deposition, synthesis of nanoparticles, metallic atomic beam source for accelerators, and probing neutral atomic beam in plasma environment (Chrisey & Hubler, 1994; Geohegan *et al.*, 1998; Doria *et al.*, 2004; Fazio *et al.*, 2009; Hoffman, 2009; Huber *et al.*, 2005; Masnavi *et al.*, 2006; Nardi *et al.*, 2009; Sizyuk *et al.*, 2007; Wolowski *et al.*, 2007; Wang *et al.*, 2007). Several attempts have been made to optimize the expanding laser produced plasma plume by varying experimental factors like, ambient gas, focal spot size, laser pulse width, irradiance, and wavelength of ablating laser (Key *et al.*, 1983; Bulgakova *et al.*, 2000; Amoruso *et al.*, 2003; Harilal, 2007; Beilis, 2007; Laska *et al.*, 2008; Rafique *et al.*, 2008). General observation is that the lateral velocity of the plume species increases with the increase in the laser fluence. Besides this, the plume expansion becomes cylindrical in shape with the increase in the laser spot size.

Address correspondence and reprint requests to: Ajai Kumar, Institute for Plasma Research, Bhat, Gandhinagar-382 428, India. E-mail: ajai@ipr.res.in, ajaiipr@yahoo.com

Plasma plume formed by laser-blow-off (LBO) technique (Adrian *et al.*, 1987; Bakos *et al.*, 1992; Veiko *et al.*, 2006; George *et al.*, 2009; Kumar *et al.*, 2010), where the laser beam interacts with a thin film of target material supported on a thick transparent substrate, is used to generate short bursts of high intensity, neutral atomic/ionic beams. This technique is extensively used for neutral atomic beam injection in plasma as a diagnostic tool, impurity transport studies for the high temperature Tokamak plasma (Huber *et al.*, 2005) and as a source of metallic atomic beam for accelerators (Doria *et al.*, 2004).

In LBO scheme, the size, shape, and divergence of the expanding plume are highly dependent on the thickness of the film, laser spot size, and laser fluence. Numerous experimental and theoretical studied have been made to address the effect of film thickness and laser fluence on the LBO generated beam (Adrian *et al.*, 1987; Baseman & Froberg, 1989; Singh *et al.*, 2007). However, little attention has been paid toward investigating the role of the intensity profile of laser beam on the geometrical aspect of the LBO plume (Schultze & Wagner, 1991) and its dynamics, which are highly relevant in thin film deposition, neutral beam injection in plasma environment, and other LBO induced beam applications.

In view of the above, we have conducted a systematic experiment to understand the expansion dynamics of the LBO plume formed by two different laser systems having

different intensity profiles *viz* Gaussian and top-hat. The LiF-C target is selected due to its application in Tokamak plasma diagnostics. Neutral atomic beam of lithium atom is advantageous for injection as a diagnostic tool due to its low atomic number (power radiated due to emission is small) and simplicity of its emission spectra (all the emission lines from ground states lie in visible region). In this report, emphasis is given to the comparison of the shape, size, directionality and angular divergence of the LBO plume observed with two different laser profiles by fast time resolved imaging spectroscopy.

EXPERIMENTAL SET-UP

A detailed description of experimental set-up has been reported in our previous papers (Singh *et al.*, 2007). Only the main features and additional parts are briefly summarized. The experiment has been carried out in a cylindrical stainless steel chamber, evacuated to a base pressure $<2 \times 10^{-5}$ Torr. The target is composed of uniform layers of 0.05 mm LiF and 0.5 mm thick carbon film, deposited on a 1.2 mm thick quartz substrate.

Nd: YAG ($\lambda = 1064$ nm) lasers having two different intensity profiles, top-hat laser beam profile (referred as "THP") of 8 ns pulse width and Gaussian beam profile (referred as "GP") of 5 ns, are used in the present study. Intensity profiles for both lasers are shown in Figure 1. The spot size of the laser beam is $\sim$1 mm diameter at the target. By adjusting the operating parameters of the laser, fluence $\sim$20 J/cm^2 is set at the target surface for both lasers. An intensified charge-coupled device (ICCD) camera (4 Picos, Stanford Computer Optics, Inc., Berkeley, CA) having variable gain and gating on time, has been used to record the time resolved images of the plume luminescence in the spectral range of 350–750 nm. In the present experiment, gate opening (integration) time is set at 4 ns. Temporal evolution of the LBO plume has been obtained by varying the time delay (from 100 to 4000 ns) between the laser pulse and the opening time of ICCD gate. Five images are recorded under similar experimental conditions. These images are found to be nearly identical in shape and the reproducibility of the emission intensity is better than 5%. A mesh image of known dimensions has been recorded in order to map the geometrical parameters of the plume. Length and full-width at half maximum of the plume are estimated by segmentation algorithm using MATLAB (Natick, MA). For better visibility, gray images have been converted into pseudo-color images using jet color map.

In order to measure the distributions of ablated ions across the expansion axis, an electrical ion probe is mounted in front of the plume propagation direction. The ion probe is constructed with tungsten wire of 0.4 mm diameter. The length of the probe, which is exposed to the plasma and separation between the probe and target plate are set as 3 mm and 45 mm, respectively. In order to get the better spatial resolution (in transverse direction), orientation of the probe is aligned along the axis of plume expansion. The probe assembly is mounted on a linear motion feed-through, which enables the positioning of probe perpendicular to the plume expansion axis. A negative bias voltage (22 V) is applied to the probe to measure the ion current in the saturation limit. A 2 μF capacitor is used to decouple the measuring circuit from the applied bias voltage. The ion signal across the 50 Ω resistance is recorded on a fast digital oscilloscope.

RESULTS AND DISCUSSION

Fast imaging of the electronically excited plume species, driven by collisional processes between electrons, ions, and neutrals generated by laser-film interaction provides the two-dimensional snap shot of the expanding LBO plume. Expansion dynamics of the species as well as geometrical aspect of the expanding plume (e.g., local structure, directionality, and divergence) can be studied by observing these emissions as a function of time. Typical ICCD images of expanding plume formed by THP and GP lasers in vacuum and at various time delays are shown in Figure 2. Each image represents spectrally integrated emission intensity in the region 350–750 nm emitted from different plume species and is normalized to the maximum intensity. A visual examination of the plume images reveals following interesting effects.

For both laser beam profiles, plume expands linearly, and their intensities diminish gradually with time. The plume expansion in vacuum under the influence of pressure gradient inside ablated plume is treated as adiabatic expansion (Singh & Narayan, 1990), where the thermal energy of plume species is rapidly converted into the kinetic energy. This leads to decrease in electron temperature and density with time and hence decrease in electron impact process (George *et al.*, 2009). Therefore, considerable reduction in the emission intensity of the plume with increase in the time delay can be anticipated. Moreover, linear dependence of the plume front position with time delay confirms free expansion of the plume (Fig. 3). Average translational velocities of 1.8×10^6 and 1.1×10^6 cm/s for the plume by THP and GP lasers, respectively, are obtained from the slopes of the curve.

However, it is observed that the lifetime of the emissive plume, directionality (divergence) and shape are highly dependent on the intensity profile of the laser beam. In case of THP, the plume is ellipsoidal in shape, i.e., the velocity component along the expansion axis is larger than the lateral one. The recorded images for THP show a non-uniform intensity pattern parallel to the direction of the plume expansion and are more intense at the leading edge of the plume and at points closer to the target. During the expansion, emission intensity decreases rapidly and finally becomes highly diffused after $>$1500 ns and is almost beyond the detection limit of the ICCD.

https://doi.org/10.1017/S0263034610000339 Published online by Cambridge University Press

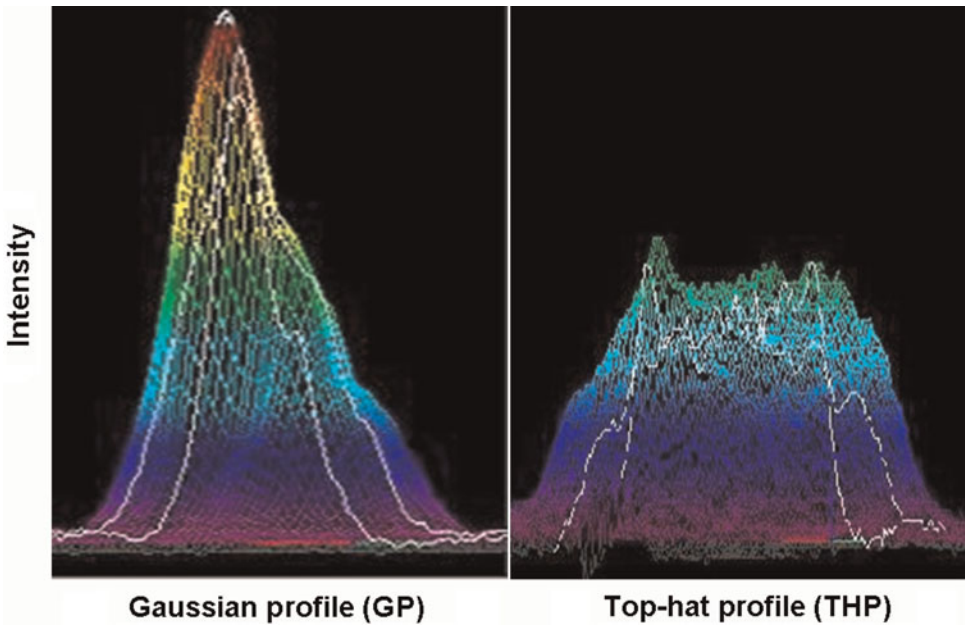

Fig. 1. (Color online) Recorded intensity profiles of laser; Gaussian beam profile, "GP" and top hat profile, "THP."

On the other hand, plume formed by GP laser expands linearly with smaller lateral velocity in comparison to that observed with THP laser. In this case, plume has nearly cylindrical shape. Moreover, the lifetime of the emissive plume is found to be significantly larger and is clearly visible up to $t > 4000$ ns. Unlike THP produced plume, it has a uniform intensity distribution; of course, it has bright patches at leading and trailing edges of the plasma. Another noteworthy observation is that the overall integrated intensities in the vertical section ($\Delta z = 0.5$ mm) of plumes produced by THP and GP laser are nearly the same (within 5% uncertainty) at any fixed location of the plume. However, due to confined geometry, images with GP laser look brighter as compared to THP-plume.

The difference in lateral expansion for these cases is clearly visible in plume width *versus* time plot as shown in Figure 4. In case of THP laser, width of the plume gradually increases with time. On the other hand, plume width with GP laser slowly increases up to $t = 2500$ ns and attains nearly constant value with further increase in the time delay. Figure 4 shows that the transverse velocity of THP plume is higher than the transverse velocity of GP plume in the overlapping region; and after $t > 2500$ ns, GP plume follows one-dimensional motion with negligible transverse velocity component.

Visible inspection of Figure 2 reveals that there is a significant difference in the divergence of the expanding plume formed by THP and GP lasers. The divergence of plume

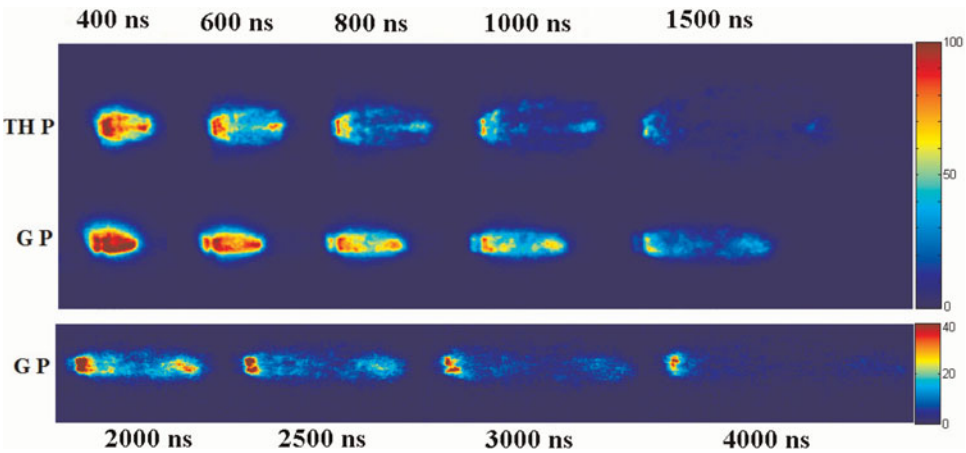

Fig. 2. (Color online) The sequence of images of expanding LBO plume in vacuum formed by THP and GP laser at different time delays. The integration time of ICCD was fixed as 4 ns. Color bar shows the normalized intensity in arbitrary unit.

https://doi.org/10.1017/S0263034610000339 Published online by Cambridge University Press

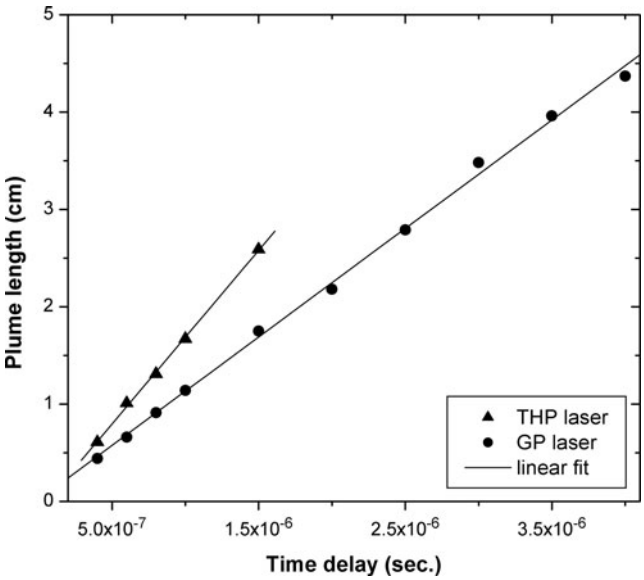

Fig. 3. Observed plume length versus time plot for the THP and GP laser generated plumes. The solid lines represent the linear fit for the experimental data.

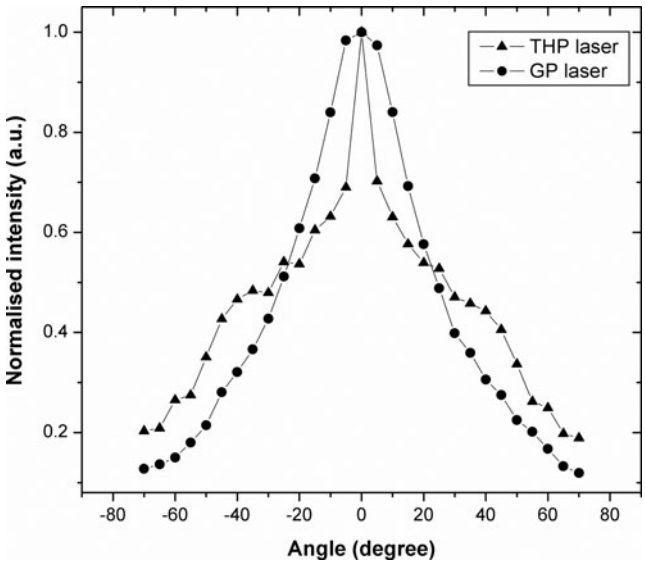

Fig. 5. Angular dependence of emission intensity of the LBO plumes produced by THP and GP laser at 800 ns time delay.

can be estimated by measuring the diameter of the plume at two separate points d_i and d_f separated by a distance x and using the relation,

$$divergence = 2\tan^{-1}\left(\frac{d_f - d_i}{2x}\right).$$

In this regard, we have selected one set of plume formation at $t = 800$ ns; and considered the portion of the plume up to the maximum acquired diameter (nearly up to half of the total length of the plume). Diameter of the plume at different locations of the plume and separation between them are used to estimate the divergence of plume for both laser systems. The estimated values of divergence of plumes formed by THP and GP lasers at $t = 800$ ns are 1.5 rad and 40 mrad, respectively. This indicates that transverse expansion in case of THP produced plume is larger in comparison to GP-plume by a factor of ~40. The measured divergence (40 mrad) with GP laser further reduces at later stages ($t > 2500$ ns) where the plume width is almost invariant with time. This is an important finding in the sense that GP produces low divergence and long lived highly collimated plume. The persistence of low divergence for the longer times is highly suitable for producing collimated atomic/ionic beams.

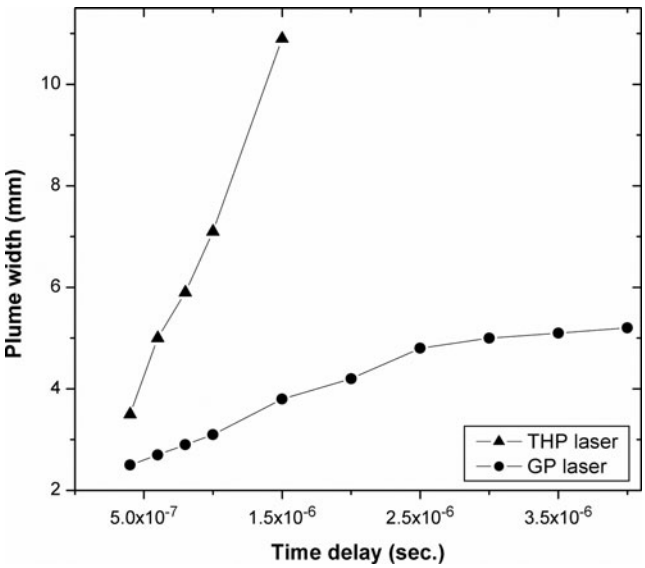

Fig. 4. Variation of plume width as a function of time delay for the both THP and GP laser.

Further, while comparing the directionality of THP and GP laser induced plumes; it is worthwhile to see the angular dependence of ejected species in the respective plumes extracted from the recorded images (Amoruso *et al.*, 2006). The recorded image is divided into radial slices (of specific width) and the emission intensity is integrated along each axis. A typical intensity distribution (normalized to its maximum) of LBO plumes formed by THP and GP laser, respectively, at a time delay, $t = 800$ ns is shown in Figure 5. It should be noted that, the difference in angular distributions for THP and GP is not as prominent as observed in visible inspection of the plume images, shown in Figure 2. This discrepancy is due to the limitation of adopted method, where the major portion of the angular slice is lying in the intense portion of the plume (close to the target), especially at higher angles, which gives wrong information at these angles. In spite of this, some features are still comparable for these two cases and we have observed some differences as well. For both cases, one can see that distribution of species is highly peaked in the forward direction

https://doi.org/10.1017/S0263034610000339 Published online by Cambridge University Press

and shows isotropic behavior. Almost similar distributions are observed for different time delays. The intensity distribution profile of THP plume appears to have two types of distributions (1) a narrow one lying near the central position and (2) a broader one appearing as a shoulder. On the other hand, species in the GP-plume lie in the narrow angular region and vary smoothly with the angle of incidence.

Since the ICCD images provide the information about the excited plume species, it is worthwhile to verify the above results with other diagnostic techniques. In this regard, the ion distributions across the expansion axis have been measured using electrical ion probe. The total intensity of ions at any probe position is obtained by the area under the temporal profile of ion current. The normalized (with maximum intensity) intensity variation of ejected ions as a function of radial distance for both THP and GP lasers are shown in Figure 6. Figure 6 clearly shows that the ion distribution is peaked in forward direction for both the laser systems and also the ions formed by GP laser have narrow distribution as compared to that of THP laser. Thus, the ion probe results further support the fact that the plume formed by GP laser is of low divergence.

It is mentioned earlier that THP plume having large divergence in comparison to plume formed by GP laser. For similar power density range, Singh and Narayan (1990) and others (Anisimov & Luk'yanchuk, 2002) have modeled the plume formation and its expansion for the conventional solid ablation. According to their proposed models, the pressure driven acceleration is larger along the direction where the plume has smaller size. Since at the initial stage, plume size along the expansion direction is small. Therefore, the velocity component along the expansion axis is much larger than the lateral one and hence the plume acquires an ellipsoidal shape. We have also observed that plume shape during expansion is elliptical as in case of THP, which is in close agreement with the proposed model. However, plume shape is close to cylindrical for GP plume. The plume size in the transverse direction varies negligibly with time (especially at higher time delays), which could not be fully predicted by the above model. This difference in the divergence of both plumes during their expansion should be related to the difference in plume formation (discussed below).

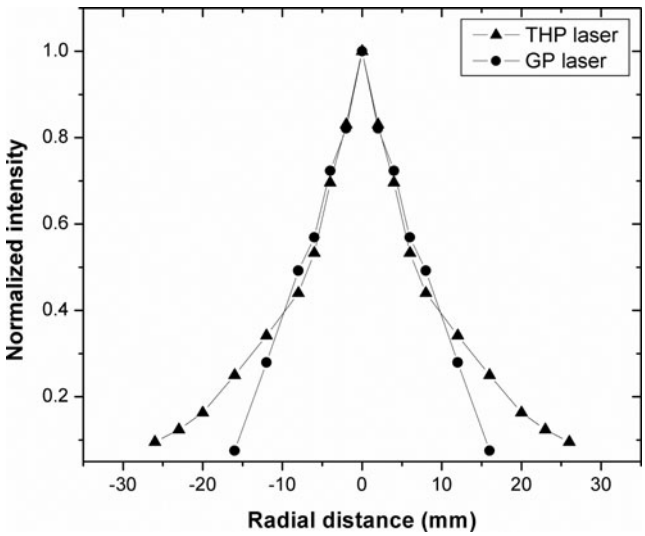

Fig. 6. Ion distributions of the LBO plumes as function of radial distance for the both THP and GP laser. The distance between the ion probe and target plate is set as 45 mm.

The GP-plume moves with smaller velocity as compared to the THP-plume, which can be understood in terms of a qualitative mechanism for the sequence of the processes in the formation of the LBO plume (Adrian *et al.*, 1987) e.g., melting of the film after the laser strikes the front surface, propagation of the melt front toward the back surface and propelling of the material due to increased vapor pressure. In case of thin film target (skin depth attaining time $<$laser pulse duration), all these events are completed before the termination of laser pulse. Therefore, the propelled material further interacts with the laser and forms the plasma plume. The time required for the melt through (melt front reaches the back surface), plays an important role in the removal process, which should depend on the power density of the laser, thickness and thermal properties of the target film.

In case of THP laser, uniform heating of target film within the irradiated region is expected. For the considered power density, the super-heated front surface having high vapor pressure causes explosive rupture of the vacuum-film interface. Therefore, the propelled material is propagated in the forward direction with significant transverse velocity component. On the other hand, in case of GP produced plume, a non-uniform heating/melting of the film favors bubble formation in between the substrate-film interface (Broer & Vriens, 1983). With increase in vapor pressure, ultimately an opening may be formed to release the material rather than the occurrence of explosive rupture. Since peak intensity of the GP laser is higher than the intensity of the THP, a smaller region of the film near the Gaussian peak will reach melt through rapidly and propulsion may start through a small area. This will reduce the buildup of vapor pressure. Therefore, the material removal will take place through a small orifice similar to gas expansion through a smaller size nozzle but with less stagnation pressure, which may result in a relatively low velocity collimated plume with GP.

SUMMARY

The reported results clearly show the dependence of characteristic expansion of the LBO plume on the laser beam intensity profile. The geometrical shape, velocity, and directionality of the plumes formed by the GP and THP laser are significantly different. One of the important observations reported in the present work is very low divergence plume produced by GP in comparison to the plume generated by THP. The results obtained by the ion probe also support the above observations. The present observations are explained on the basis of the

https://doi.org/10.1017/S0263034610000339 Published online by Cambridge University Press

existing models; however more theoretical work is required to understand it quantitatively. Nonetheless we feel that present observations will be of significant importance in shaping laser generated plasma plumes and understanding and controlling the geometrical aspect of the LBO generated atomic/ionic beam.

REFERENCES

Adrian, F.J., Bohandy, J., Kim, B.F., Jette, A.N. & Thomson, P. (1987). A study of the mechanism of metal deposition by the laser-induced forward transfer process. *J. Vac. Sci. Technol. B* **5**, 1490–1494.

Amoruso, S., Bruzzese, R., Spinelli, N., Velotta, R., Vitiello, M. & Wang, X. (2003). Dynamics of laser-ablated MgB_2 plasma expanding in argon probed by optical emission spectroscopy. *Phys. Rev. B* **67**, 224503–1/224503–11.

Amoruso, S., Sambri, A. & Wang, X. (2006). Propagation dynamics of a $LaMnO_3$ laser ablation plume in an oxygen atmosphere. *J. Appl. Phys*. **100**, 013302–1/013302–11.

Anisimov, S.I. & Luk'yanchuk, B.S. (2002). Selected problems of laser ablation theory. *Phys. Uspekhi* **45**, 293–324.

Bakos, J.S., Földes, I.B., Ignácz, P.N., Kedves, M.A. & Szigeti, J. (1992). Radiation imprisonment in laser blow-off plasma. *Laser Part. Beams* **10**, 715–721.

Baseman, R.J. & Froberg, N.M. (1989). Time-resolved transmission of thin gold films during laser blow-off. *Appl. Phys. Lett*. **55**, 1841–1843.

Beilis, Isak I. (2007). Laser plasma generation and plasma interaction with ablative target. *Laser Part. Beams* **25**, 53–63.

Broer, D.J. & Vriens, L. (1983). Laser-induced optical recording in thin films. *Appl. Phys. A* **32**, 107–123.

Bulgakova, N.M., Bulgakov, A.V. & Bobrenok, O.F. (2000). Double layer effects in laser-ablation plasma plumes. *Phy. Rev. E* **62**, 5624–5635.

Chrisey, D.B. & Hubler, G.K. (1994). *Pulsed Laser Deposition of Thin Films*. New York: John Wiley & Sons.

Doria, D., Lorusso, A., Belloni, F., Nassisi, V., Torrisi, L. & Gammino, S. (2004). A study of the parameters of particles ejected from a laser plasma. *Laser Part. Beams* **22**, 461–467.

Fazio, E., Neri, F., Ossi, P.M., Santo, N. & Trusso, S. (2009). Ag nanocluster synthesis by laser ablation in Ar atmosphere: A plume dynamics analysis. *Laser Part. Beams*, **27**, 281–290.

Geohegan, D.B., Puretzky, A.A., Duscher, G. & Pennycook, S.J. (1998). Photoluminescence from gas-suspended SiO_x nanoparticles synthesized by laser ablation. *Appl. Phys. Lett*. **73**, 438–440.

George, Sony., Kumar, Ajai., Singh, R.K. & Nampoori, V.P.N. (2009). Fast imaging of laser-blow-off plume: Lateral confinement in ambient environment. *Appl. Phys. Lett* **94**, 141501–1/141501–3.

Harilal, S.S. (2007). Influence of spot size on propagation dynamics of laser-produced tin plasma. *J. Appl. Phys*. **102**, 123306–1/123306–6.

Hoffman, D.H.H. (2009). Ion and laser beams as tools for high energy density physics. *Laser Part. Beams*, **27**, 1–2.

Huber, A., Samm, U., Schweer, B. & Mertens, Ph. (2005). Result from a double Li-beam technique for measurement of both radial and poloidal components of electron density fluctuations using two thermal beams. *Plasma Phys. Contr. Fusion* **47**, 409–440.

Key, M.H., Toner, W.T., Goldsack, T.J., Kilkenny, J.D., Veats, S.A., Cunningham, P.F. & Lewis, C.L.S. (1983). A study of ablation by laser irradiation of plane targets at wavelengths 1.05, 0.53, and 0.35 μm. *Phys. Fluids* **26**, 2011–2026.

Kumar, Ajai., Singh, R.K., Prahlad, V. & Joshi, H.C. (2010). Effect of magnetic field on the Laser-Blow-Off of Li plasma: Role of atomic processes. *Laser Part. Beams*. **28**, 121–127.

Laska, L., Jungwirth, K., Krasa, J., Krousky, E., Pfeifer, M., Rohlena, K., Velyhan, A., Ullschmied, J., Gammino, S., Torrisi, L., Badziak, J., Parys, P., Rosinski, M., Ryc, L., & Wolowskim, J. (2008). Angular distributions of ions emitted from laser plasma produced at various irradiation angles and laser intensities. *Laser Part. Beams* **26**, 555–565.

Masnavi, M., Nakajima, M., Sasaki, A., Hotta, E. & Horioka, K. (2006). Potential of discharge-based lithium plasma as an extreme ultraviolet source. *Appl. Phys. Lett*. **89**, 031503–1/031503–3.

Nardi, E., Maron, Y. & Hoffmann, D.H.H. (2009). Dynamic screening and charge state of fast ions in plasma and solids. *Laser Part. Beams*, **27**, 355–361.

Rafique, M.S., Khaleeq-Ur-Rahman, M., Riaz, I., Jalil, R. & Farid, N. (2008). External magnetic field effect on plume images and X-ray emission from a nanosecond laser produced plasma. *Laser Part. Beams*, **26**, 217–224.

Schultze, V. & Wagner, M. (1991). Blow-off of aluminum films. *Appl. Phys. A* **53**, 241–248.

Singh, R.K. & Narayan, J. (1990). Pulsed-laser evaporation technique for deposition of thin films: Physics and theoretical model. *Phys. Rev. B* **41**, 8843–8859.

Singh, R.K., Kumar, Ajai., Patel, B.G. & Subramanian, K.P. (2007). Role of ambient gas and laser fluence in governing the dynamics of the plasma plumes produced by laser blow off of LiF–C thin film. *J. Appl. Phys*. **101**, 103301–1/103301–9.

Sizyuk, V., Hassanein, A. & Sizyuk, T. (2007). Hollow laser self-confined plasma for extreme ultraviolet lithography and other applications. *Laser Part. Beams* **25**, 143–154.

Veiko, V.P., Shakhno, E.A., Smirnov, V.N., Miaskovski, A.M. & Nikishin, G.D. (2006). Laser – induced film deposition by LIFT: Physical mechanisms and applications. *Laser Part. Beams* **24**, 203–209.

Wang, Y-L., Xu, W., Zhou, Y., Chu, L-Z. & Fu, G-S. (2007). Influence of pulse repetition rate on the average size of silicon nanoparticles deposited by laser ablation. *Laser Part. Beams* **25**, 9–13.

Wolowski, J., Badziak, J., Czarnecka, A., Parys, P., Pisarek, M., Rosinski, M., Turan, R. & Yerci, S. (2007). Application of pulsed laser deposition and laser-induced ion implantation for formation of semiconductor nano-crystallites. *Laser Part. Beams* **25**, 65–69.